

V. CONCLUSION

The topological automaton model provides an interesting extension of the standard cellular automaton. Changes in topological structure and in dimensionality can more easily be described by the newer model. It is hoped that topological automata will provide insights into the dynamics of physical systems, including statistical models of gases and crystals, and theories of particle interaction.

ACKNOWLEDGMENTS

The author wishes to thank A. Ilachinski for introducing him to the topological automaton model, and P. Millet for suggesting this article.

^{a)} Current address: Department of Mathematics and Physics, Philadelphia College of Pharmacy and Science, 43rd Street and Woodland Avenue, Philadelphia, PA 19104.

¹J. H. Conway (unpublished, 1970).

²M. Gardner, *Sci. Am.* **223**, 120 (1970).

³S. Wolfram, *Rev. Mod. Phys.* **55**, 601 (1983).

⁴N. Packard, "Cellular automaton models for dendritic crystal growth," Institute for Advanced Studies preprint (1985).

⁵N. Packard and S. Wolfram, *J. Stat. Phys.* **38**, 901 (1985).

⁶D. W. Thompson, in *On Growth and Form*, edited by J. T. Bonner (Cambridge U. P., New York, 1961), abridged ed.

⁷P. S. Stevens, *Patterns in Nature* (Little, Brown, Boston, 1974).

⁸A. Ilachinski, "Topological life-games I," Stony Brook preprint (1986).

⁹A. Ilachinski and P. Halpern, *Complex Syst.* **1**, 503 (1987).

¹⁰P. Halpern, "Long term behavior of topological cellular automata," submitted to *J. Stat. Phys.*

¹¹W. K. Clifford, in *Lectures and Essays*, edited by L. Stephen and F. Pollack (MacMillan, London, 1879).

¹²J. A. Wheeler, *Geometrodynamics* (Academic, New York, 1962).

¹³C. W. Misner, K. S. Thorne, and J. A. Wheeler, *Gravitation* (Freeman, San Francisco, 1973).

¹⁴G. J. Whitrow, *Natural Philosophy of Time* (Harper & Row, New York, 1961).

¹⁵T. D. Lee, *Phys. Lett.* **122B**, 216 (1982).

¹⁶P. Rujan, *J. Stat. Phys.* **49**, 139 (1987).

¹⁷P. Grassberger, *J. Stat. Phys.* **45**, 27 (1986).

Nonlinear and chaotic string vibrations

Nicholas B. Tufillaro

Department of Physics, Bryn Mawr College, Bryn Mawr, Pennsylvania 19010

(Received 10 February 1988; accepted for publication 21 June 1988)

The nonlinear vibrations of an elastic string are studied. A string is capable of showing nonlinear phenomena including periodic, quasiperiodic, and chaotic motions. Hysteresis is found using the method of slowly varying amplitudes, and chaotic vibrations are predicted for an experimentally accessible regime.

I. INTRODUCTION

Like a jump rope, strings tend to swing in a circle, a fact well known to children and laboratory instructors.¹ When both ends are fixed, it is often difficult to drive a string so that motion is confined to a single transverse plane. Borrowing terminology from optics, we would say that a string prefers circular polarization to plane polarization. If the string mounts are symmetric, then there is no preferred plane of polarization. Musical instruments, however, often use a bridge that breaks this symmetry leading to horizontal and vertical polarizations possessing very different decay rates.^{2,3} In addition to whirling, several other interesting phenomena are easily observed in such forced strings, including periodic and *aperiodic* cycling between large and small amplitude motions.

When a string vibrates, the length of the string must also fluctuate, causing oscillations in the string's tension. These longitudinal oscillations occur at about twice the frequency of the transverse vibrations. The coupling between transverse and longitudinal string oscillations is essentially a nonlinear phenomenon that is not captured by the familiar linear model. This coupling was first analyzed by Rayleigh,⁴ who was attempting to explain Melde's experiment,

which showed that a strictly longitudinal periodic forcing gives rise to a transverse vibration when the period of forcing is twice one of the modal frequencies.

Several authors⁵⁻⁷ argue that string oscillations are properly modeled by *nonlinear equations even when the transverse displacement is small*. In the linear model, it is assumed that the longitudinal displacement of the string is everywhere zero. This assumption, along with the small transverse oscillation assumption, leads to the linear wave equation. However, if both the longitudinal (i.e., tension) and transverse displacements are small, then the simplest model of a string is necessarily nonlinear. This point is demonstrated by Narasimha,⁶ who shows that it is neither necessary nor justifiable to assume that there is no variation in tension.

Thus strings, like lasers and hydrodynamic systems, are essentially nonlinear oscillators and should exhibit multiple coexisting solutions (attractors), hysteresis, harmonic distortion, periodic, quasiperiodic, and chaotic attractors.⁸

Nonlinear systems, and in particular systems with spatial distribution, are currently receiving considerable theoretical and experimental attention. Spatial-temporal chaos (turbulence) and pattern formation in far from equilibrium systems are the central problems being investigated.

The elastic string is easily one of the simplest spatially distributed nonlinear systems imaginable; in addition to its intrinsic theoretical interest, the dynamics of a nonlinear elastic string could shed light onto the dynamics of more complicated systems such as lasers. Theoretical studies of nonlinear strings are simpler and more analytically tractable than those of lasers and hydrodynamic systems. More importantly, experimental spatial-temporal studies of string vibrations are relatively easy and inexpensive to perform using optical detection schemes.⁹ Nonlinearity in strings can also lead to important acoustical effects of practical interest to musicians, instrument makers, and acoustical engineers. For instance, Gough¹⁰ has shown that nonlinearity can lead to the modulation of sounds from a cello or a guitar, and that the whirling motion accounts for the rattling heard when a string is strongly plucked or bowed.

In this article, we will study a very simple single-mode model of string vibrations, which is a straightforward extension of the nonlinear oscillator studied by Morse and Ingard.⁵ This single-mode model gives rise to a set of coupled differential equations that were previously deduced by several authors with methods of varying rigor.¹¹⁻¹³ Our simple picture, however, allows us to arrive at the single-mode model in a very economical way, and the equations thus derived are identical with those that arise from the more cumbersome single-mode truncations of multimode models. In addition, all the constants in the single-mode model are easy to obtain from parameters in actual experiments. In Secs. III-V, we undertake a systematic investigation of the single-mode model for both plane and circularly polarized motions in the free and forced cases. Calculations presented in these sections are mostly a summary of results scattered throughout the literature. In Sec. VI, we observe that the vibrating string can oscillate chaotically and we proceed with the initial numerical studies to indicate under what experimental circumstances instabilities and chaotic oscillations should be observable.

This article, therefore, offers the first steps toward a comprehensive theory of nonlinear and chaotic behavior in vibrating strings. The relative ease with which strings can be studied both theoretically and experimentally makes them ideal candidates for current studies in nonlinear dynamics.

II. SINGLE-MODE MODEL

A simple model of a string oscillating in its fundamental mode is presented in Fig. 1. The ends of a massless spring are fixed a distance l apart where the relaxed length of the spring is l_0 and the spring constant is k . To the center of the spring a mass is attached that is free to make oscillations in the x - y plane centered at the origin. The mass is subject to damping and forcing. For example, if the mass is composed of steel, it can be driven by an oscillating magnetic field. Note that motion in the two transverse directions— x and y —is coupled directly, and also indirectly via the longitudinal motion of the spring. Both of these coupling mechanisms are nonlinear. The multimode extension of the simple model would, in addition, possess nonlinear couplings among the normal modes of the linear problem.

The restoring force on the mass shown in Fig. 1 is

$$F = -4kr(1 - l_0/\sqrt{l^2 + 4r^2}), \quad (1)$$

where the position of the mass is given by polar coordinates (r, θ) of the transverse plane. Expanding the left-hand side

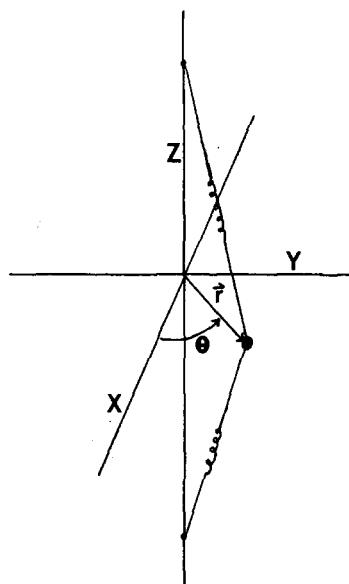


Fig. 1. Single-mode model for nonlinear string vibrations. String vibrations are assumed to be in the fundamental mode and are measured in the transverse x - y plane by the polar coordinates (r, θ) .

of Eq. (1) in a series ($r < l$), we find that

$$F = -kr(l - l_0)\left(\frac{r}{l}\right) - 8kl_0\left[\left(\frac{r}{l}\right)^3 - 3\left(\frac{r}{l}\right)^5 + \dots\right],$$

which can be approximated by

$$F = m\ddot{r} \approx -4k(l - l_0)\left(\frac{r}{l}\right)\left[1 + \frac{2l_0}{(l - l_0)}\left(\frac{r}{l}\right)^2\right], \quad (2)$$

a cubic restoring force. Notice the nonlinearity dominates when $l \approx l_0$.

Defining

$$\omega_0^2 \equiv (4k/m)[(l - l_0)/l], \quad (3)$$

and

$$K \equiv 2l_0/l^2(l - l_0). \quad (4)$$

Then, from Eq. (2), we get

$$\ddot{r} + \omega_0^2 r(1 + Kr^2) = 0, \quad (5)$$

the equation of motion for a two-dimensional conservative cubic oscillator. The behavior of Eq. (5) depends critically upon the ratio (l_0/l) . If $l_0 < l$, the equilibrium at $r = 0$ is stable and we have a model for a string vibrating primarily in its fundamental mode. On the other hand, if $l_0 > l$, then the origin is an unstable equilibrium point, and two stable equilibrium points exist at approximately $r = \pm l$. This latter case models an elastic beam. For our purpose, we will only study the case $l_0 < l$, i.e., $K > 0$.

In general, we will want to consider damping and forcing so Eq. (5) is modified to read

$$\ddot{r} + \lambda\dot{r} + \omega_0^2(1 + Kr^2)r = f(\omega t), \quad (6)$$

where $f(\omega t)$ is a forcing term and λ is the damping coefficient. In this article, we assume that the ends of the string are symmetrically fixed, so that λ is a scalar.

Equation (5) is also derived by Gough¹⁰ and Elliot,^{11,14} both of whom relate ω_0 and K to actual string parameters. For instance, Gough shows that

$$\omega_0^2 = c\pi/l, \quad (7)$$

and

$$K = (1/\epsilon l)(\pi/2)^2, \quad (8)$$

where ϵ is the longitudinal extension of a string of length l , ω_0 is the low-amplitude angular frequency of free vibration, and c is the transverse wave velocity. Again, we see that the nonlinearity parameter K increases as the longitudinal extension ϵ approaches zero. That is, the nonlinearity is enhanced when the longitudinal extension—and hence the tension—is small. Nonlinear effects are also amplified when the overall string length is shortened. For a Jargar viola D string with a vibration amplitude of 1 mm, typical values of the string parameters showing nonlinear effects are: $l = 27.5$ cm, $\omega_0 = 60$ Hz, $\epsilon = 0.079$ mm, and $K = 0.128 \text{ mm}^{-2}$.¹⁰

Equation (6) constitutes our single-mode model for nonlinear string vibrations and is the central result of Sec. II. For some calculations, it will be advantageous to write Eq. (6) in dimensionless form. To this end, consider the transformation

$$\tau = \omega_0 t, \quad \mathbf{s} = \mathbf{r}/l_0, \quad (9)$$

giving

$$\mathbf{s}'' + \beta \mathbf{s}' + (1 + \alpha \mathbf{s}^2) \mathbf{s} = \mathbf{g}(\gamma \tau), \quad (10)$$

where the prime denotes differentiation wrt τ and

$$\beta \equiv \lambda/\omega_0, \quad \alpha \equiv Kl_0^2, \quad \mathbf{g} \equiv \mathbf{f}/l_0\omega_0^2, \quad \text{and} \quad \gamma \equiv \omega/\omega_0. \quad (11)$$

Before we begin a systematic investigation of the single-mode model, it is useful to look at the unforced— $\mathbf{f}(\omega t) = 0$ —linear problem. If the nonlinearity parameter K is small, then Eq. (6) is simply a two-degree-of-freedom linear harmonic oscillator with damping, which admits solutions of the form

$$\mathbf{r} = (A \cos \omega_0 t, B \sin \omega_0 t) e^{-\lambda t/2}. \quad (12)$$

In the conservative limit ($\lambda = 0$), the orbits are ellipses centered about the z axis. As we shall show later, one effect of the nonlinearity is to cause these elliptical orbits to precess.

III. EXACT SOLUTIONS FOR CIRCULAR AND PLANAR MOTION

The free conservative oscillator of Eq. (5) admits exact solutions in two special circumstances. The first is the case of circular motion at a constant radius R . In Fig. 1, we could imagine circular orbits arising when the restoring force just balances the centrifugal force. Plugging the ansatz

$$\mathbf{r} = (R \cos \omega t, R \sin \omega t) \quad (13)$$

into Eq. (5), we see that it is indeed a solution provided the frequency is adjusted to

$$\omega_c^2 = \omega_0^2 (1 + KR^2). \quad (14)$$

The second solution appears when we consider planar motion. If all the motion is confined to the x - z plane, then the system is a single-degree-of-freedom oscillator whose equation of motion in the dimensionless form obtained from Eq. (10) is

$$x'' + x + \alpha x^3 = 0. \quad (15)$$

The exact solution to Eq. (15) is,¹⁵

$$\tau = \frac{1}{(1 + 4\alpha E)^{1/4}} \times \left[I \left(\frac{a^2}{a^2 + b^2} \right) - J \left(\arccos \frac{x}{a}, \frac{a^2}{a^2 + b^2} \right) \right], \quad (16)$$

where $J(\theta, \phi)$ is an elliptic integral of the first kind and $I(\phi) = J(\pi/2, \phi)$; E is the energy constant

$$E = \frac{1}{2}x'^2 + \frac{1}{2}x^2 + (\alpha/4)x^4 \quad (17)$$

and

$$b^2, a^2 = (1/\alpha)(\sqrt{1 + 4\alpha E} \pm 1). \quad (18)$$

As in circular motion, the frequency in planar motion is again shifted to a new value given by

$$\gamma_p = (\pi/2) \{ (1 + 4\alpha E)^{1/4} / I [a^2/(a^2 + b^2)] \}. \quad (19)$$

The exact solutions for circular and planar motion are useful benchmarks for testing limiting cases of more general, but not necessarily exact, results.

IV. PLANAR MOTION

Imagine that the ends of the string are fastened in such a way that the string only vibrates in a single plane. Then the nonlinear equation of motion for a string vibrating primarily in its fundamental mode is a forced Duffing equation of the form,

$$x'' + \beta x' + (1 + \alpha x^2)x = g(\gamma \tau), \quad (20)$$

where Eq. (20) is calculated from Eq. (10) by assuming that the motion is confined to the x - z plane in Fig. 1. The forcing term will generally be taken as a periodic excitation of the form

$$g(\gamma \tau) = F \cos(\gamma \tau). \quad (21)$$

The literature studying the Duffing equation is extensive, and it is well known that Eq. (20) is already complicated enough to exhibit multiple periodic solutions, quasiperiodic orbits, and chaos.¹⁶ A good guide to nonchaotic properties of the Duffing equation is the book by Nayfeh and Mook.¹⁷ Also, the book by Hayashi,¹⁸ *Nonlinear Oscillations in Physical Systems*, is highly recommended since it deals almost exclusively with Duffing's equation. In this section, we examine frequency shifts and hysteresis in the Duffing equation since these phenomena are easily observed in strings.

As a first step toward studying the Duffing equation, let us neglect the nonlinear term in Eq. (20) ($\alpha = 0$) and look at the solution to the resulting linear system with periodic forcing,

$$x(\tau) = ae^{-\beta\tau/2} \cos[(1 - \beta^2)\tau + b] + F[(1 - \gamma^2)^2 + \beta^2\gamma^2]^{-1/2} \cos(\gamma\tau + \theta). \quad (22)$$

The constants a and b are determined from initial conditions. After the transient solution dies out, the steady-state response has the same frequency as the forcing term, but it is phase shifted by an amount θ , which depends on β , γ , and F . As with all damped linear systems, the steady-state response is independent of the initial conditions so that we can speak of *the* solution.

In the linear solution, Eq. (22), large motions occur when F is large or when $\gamma \approx 1$, the normalized natural undamped frequency. A primary (or main) resonance exists when the natural frequency and the excitation frequency

are close; under these circumstances, the nonlinear term in Eq. (20) cannot be neglected. Thus, even for planar motion, a nonlinear model of string vibrations is required when a resonance occurs, or the excitation amplitude is large.

Returning to the Duffing oscillator, we generally expect that in a nonlinear system the maximum response frequency will be detuned slightly from its natural frequency. An estimate for this detuning is obtained by studying the undamped, free Duffing oscillator, by means of the method of slowly varying amplitude.¹⁹ Write

$$x(\tau) = \frac{1}{2}[A(\tau)e^{i\gamma\tau} + A^*(\tau)e^{-i\gamma\tau}] \quad (23)$$

and plug Eq. (23) into Eq. (15), while assuming $A(\tau)$ varies slowly in the sense that $|A''| \ll \omega^2 A$. Then Eq. (15) is approximated by

$$(2i\gamma)A' + [1 + \gamma^2 + (3\alpha/4)|A|^2]A = 0, \quad (24)$$

where we ignore all terms not at the driving frequency. Equation (24) has a steady-state solution denoted by \bar{A} when $A' = 0$,

$$\gamma^2 = 1 + (3\alpha/4)|\bar{A}|^2, \quad (25)$$

i.e.,²⁰

$$\bar{x}(\tau) = \bar{A} \cos(\gamma\tau). \quad (26)$$

To first order, the nonlinearity increases the normalized frequency by an amount depending on the amplitude of oscillation and the nonlinearity parameter. This approximate value for a hard Duffing oscillator is consistent with the exact result found in Sec. III.

Hysteretic effects are discovered when we apply the slowly varying amplitude approximation to the forced Duffing equation

$$x'' + \beta x' + (1 + \alpha x^2)x = F \cos(\gamma\tau). \quad (27)$$

Plugging Eq. (23) into Eq. (27) and again keeping only the appropriate terms, we arrive at the complex amplitude equation

$$(\beta + 2i\gamma)A' + [1 - \gamma^2 + i\beta\gamma + (3\alpha/4)|A|^2]A = F, \quad (28)$$

which in steady state ($A' = 0$) becomes

$$[1 - \gamma^2 + i\beta\gamma + (3\alpha/4)|\bar{A}|^2]\bar{A} = F. \quad (29)$$

To find the set of real equations for the steady state write the complex amplitude in the form

$$\bar{A} = ae^{ib}, \quad (30)$$

where both a and b are real constants. Then Eq. (29) separates into two real equations

$$\beta a = F \sin b, \quad (31)$$

and

$$[1 - \gamma^2 + (3\alpha/4)a^2]a = F \cos b, \quad (32)$$

which collectively determine both the phase and the amplitude of the response. Squaring both Eqs. (31) and (32), and then adding the results, we obtain a cubic equation in

$$\{(\beta\gamma)^2 + [1 - \gamma^2 + (3\alpha/4)a^2]\}a^2 = F^2, \quad (33)$$

illustrated in Fig. 2, which is known as the *frequency-response curve*. In this approximation, the steady-state response is given by

$$\bar{x} = a \cos(\gamma\tau - b), \quad (34)$$

which is exactly tuned to the forcing excitation but phase shifted by $-b$.

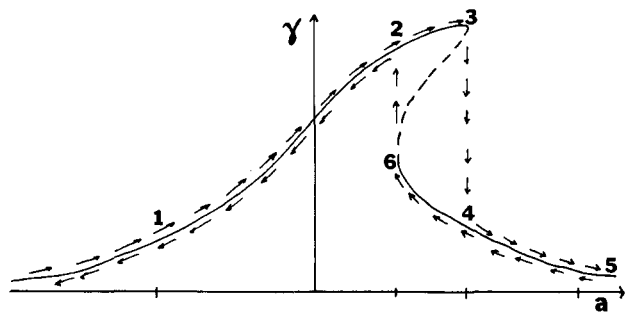


Fig. 2. Schematic frequency-response curve of a vibrating string for excitations at a primary resonance. Hysteretic effects are displayed including a jump between different steady-state responses at points 4 and 6. The dashed line indicates an unstable periodic orbit.

The frequency-response curve shown in Fig. 2 indicates that a string vibrating in a plane should—near a primary resonance—exhibit hysteresis due to the coexistence of two stable states, and that a discontinuous transition between these two states is possible when a parameter is slowly varied, the so-called *quasistatic* approximation. To see these effects, hold the excitation amplitude constant while slowly scanning through the frequency. As indicated in Fig. 2, if the frequency is increased, then the amplitude will switch to a smaller value at point 3. On the other hand, if the excitation frequency is slowly decreased, then the response amplitude will switch up at point 6. In the region between points 6 and 4, two stable periodic orbits and one unstable periodic orbit (indicated by the dashed line) all coexist.²¹ This discontinuous jumping between two stable orbits is a result of the nonlinear phase-amplitude relation [Eq. (33)] and is, in fact, an example of a fold catastrophe.²²

In a linear system with damping, the steady state is independent of the initial conditions. In contrast, the coexistence of two or more stable steady states for the same parameter values in a nonlinear system indicates that the initial conditions play a critical role in determining the system's overall response. To discover the *global* stability of an

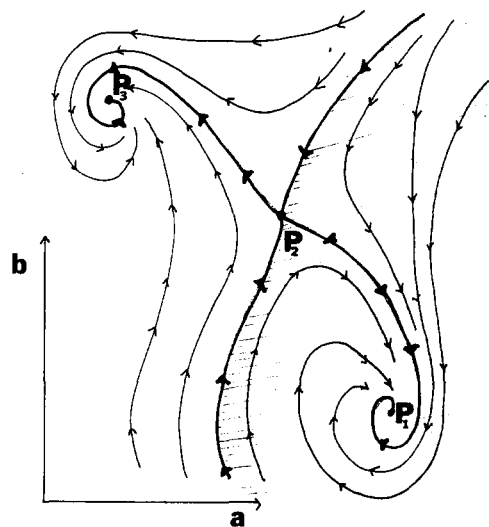


Fig. 3. Schematic phase space for Duffing's equation when two stable periodic orbits (P_1 and P_3), and one unstable periodic orbit (P_2) all coexist. The steady-state response depends critically on the initial conditions.

orbit, the domain of attraction, i.e., the so-called *basin of attraction* must be determined for the steady-state response in question. A schematic for the basins of attraction in a Duffing oscillator with three coexisting orbits is portrayed in Fig. 3. The phase space of all initial conditions shows two stable orbits P_1 and P_3 , and one unstable orbit P_2 . The shaded region shows all initial conditions that approach the orbit P_1 , while the unshaded region shows all the initial conditions that reach P_3 . In the region of P_2 , a small change in the initial conditions can produce a large change in the response of the system since it can result in two different steady-state responses. The picture for the basins of attraction shown in Fig. 3 is over simplified. In general, basins of attraction for a nonlinear system can be enormously complex, and can only be constructed by numerical simulations. Assessing the global stability of attractors in nonlinear systems is currently a subject of intense research.²³

V. CIRCULAR MOTIONS

If a free planar oscillation is perturbed, then the subsequent evolution of the orbit is determined by the two-di-

$$(\omega_0^2 - \Omega^2 - \tilde{\omega}^2)X_1 \cos \tilde{\omega}t + (\omega_0^2 - \Omega^2 - 9\tilde{\omega}^2)X_3 \cos 3\tilde{\omega}t - 2\Omega\tilde{\omega}Y_1 \cos \tilde{\omega}t + \omega_0^2 K(X_1^2 \cos^2 \tilde{\omega}t + Y_1^2 \sin^2 \tilde{\omega}t)e^{-\lambda t}X_1 \cos \tilde{\omega}t = 0. \quad (38)$$

A similar relation also holds for the y coordinate. On equating like Fourier components we discover, after considerable algebra,

$$\tilde{\omega}^2 = \omega_0^2 [1 + (3K/4)(X_1^2 + Y_1^2)e^{-\lambda t}] - \Omega^2, \quad (39)$$

$$\tilde{\omega}\Omega/\omega_0^2 = (-K/4)X_1Y_1e^{-\lambda t}, \quad (40)$$

and

$$\frac{X_3}{X_1} = \frac{Y_3}{Y_1} = \left(\frac{K}{4}\right) \frac{\omega_0^2(X_1^2 - Y_1^2)}{(9\tilde{\omega}^2 - \omega_0^2 + \Omega)}. \quad (41)$$

If there is no damping ($\lambda = 0$), then this approximate solution is periodic in the rotating reference frame and is slightly distorted from an elliptical orbit. The angular frequency $\tilde{\omega}$ is detuned from ω_0 by an amount proportional to the mean-square radius vector $X_1^2 + Y_1^2$. In the original stationary reference frame, Eq. (40) shows us that the orbit precesses at a rate Ω , which is proportional to the orbital area $\pi X_1 Y_1$. The angular frequency $\tilde{\omega}$ in Eqs. (39)–(41) is measured in the rotating reference frame. It is related to the angular frequency in the stationary reference frame ω by

$$\omega^2 = (\tilde{\omega} + \Omega)^2 = \omega_0^2 [1 + (K/4) [3(X_1^2 + Y_1^2) - 2X_1 Y_1] e^{-\lambda t}]. \quad (42)$$

Thus, in the stationary reference frame, the undamped motion is quasiperiodic unless $\tilde{\omega}$ and Ω are accidentally commensurate. The damped oscillations are also elliptical in character and precess as a rate Ω . In both cases, the detuning given by Eq. (42) is due to two sources: the nonlinear planar motion detuning plus a detuning resulting from the precessional frequency.

Solutions for forced circular motion, Eq. (6), will not be studied here, suffice it to say that the system has five degrees of freedom and will exhibit all the nonlinear and cha-

dimensional equation

$$\ddot{\mathbf{r}} + \lambda \dot{\mathbf{r}} + \omega_0^2(1 + K\mathbf{r}^2)\mathbf{r} = 0, \quad (35)$$

which is Eq. (6) with no forcing term. We noted in Sec. II that the linear approximation to Eq. (35) results in elliptical motion. We shall use this observation to calculate an approximate solution to Eq. (35) using a procedure put forth by Gough¹⁰; similar results were obtained by Elliot.¹¹

Transform the problem of nonlinear free vibrations to a reference frame rotating with an angular frequency Ω . In this rotating frame, Eq. (35) becomes

$$\ddot{\mathbf{u}} + \lambda \dot{\mathbf{u}} + 2\Omega \times \dot{\mathbf{u}} - \Omega^2 \mathbf{u} + \omega_0^2(1 + K\mathbf{u}^2)\mathbf{u} = 0, \quad (36)$$

where \mathbf{u} is the new radial displacement vector subject to the addition of a Coriolis and centrifugal acceleration. Let us now look for a solution of the form

$$\mathbf{u}(t) = [x(t), y(t)] = e^{\lambda t/2} \times (X_1 \cos \tilde{\omega}t + X_3 \cos 3\tilde{\omega}t, Y_1 \sin \tilde{\omega}t + Y_3 \sin 3\tilde{\omega}t). \quad (37)$$

Plugging Eq. (37) into Eq. (35) and keeping only the first-order corrections in X_3 and Y_3 gives

otic effects of dynamical systems of similar complexity. Equation (6) can be viewed as a set of two coupled Duffing equations. Some of the possible behavior of this system is indicated in Sec. VI, where the results from numerical simulations are presented.

VI. CHAOTIC MOTIONS

One of the simplest ways to visualize the complexity of string vibrations is through the construction of a *bifurcation diagram*.⁸ Such diagrams are useful aids in showing the transition from periodic to chaotic behavior; bifurcation diagrams can also demonstrate the existence of multiple coexisting attractors. We will construct bifurcation diagrams for forced planar motion modeled by the Duffing oscillator, Eq. (20); and the two-degree-of-freedom model for forced circular motion, Eq. (10). In each case, we assume the string is forced only in the x direction by the sinusoidal term given in Eq. (21). For all simulations, $\beta = 0.0037$, $\alpha = 86.2$ (i.e., $K = 0.114$), $\gamma = 0.99$ (i.e., a 1% detuning), and the forcing amplitude F varies between 50 and 55. All these dimensionless parameters correspond to values that should be easy to realize experimentally.

To actually construct the bifurcation diagram, the differential equations are solved numerically with ODE,²⁴ a research tool of remarkable utility. The first 400 cycles are disregarded since they are assumed to be part of the transient solution. In the next 400 oscillations, the values of $x(\tau_n)$ are recorded where $\tau_n = (\tau \bmod 2\pi = 0)$. That is, the attracting solution is sampled by the stroboscopic method once every period of forcing. The asymptotic solution is then used as the initial condition for the next simulation where the value of F is incremented by a small amount.

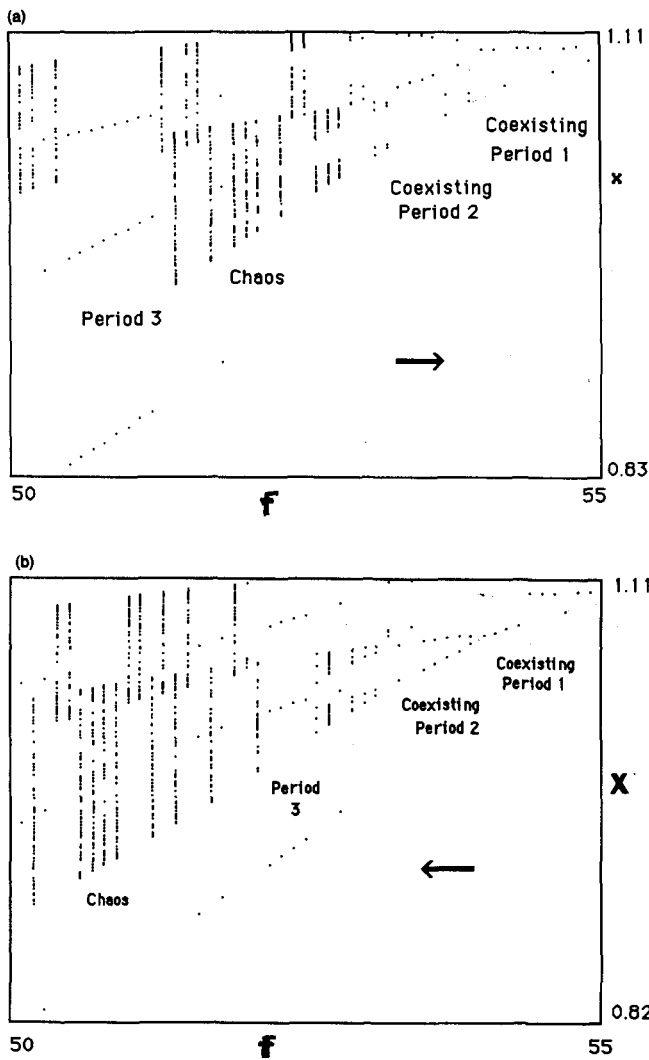


Fig. 4. Bifurcation diagram [forcing amplitude vs $x(\tau_n)$] for planar oscillations of a vibrating string: (a) forward scan, (b) backward scan. Coexisting periodic orbits and chaotic motion are easily observed. The operating parameters are $\beta = 0.0037$, $\alpha = 86.2$, and $\gamma = 0.99$.

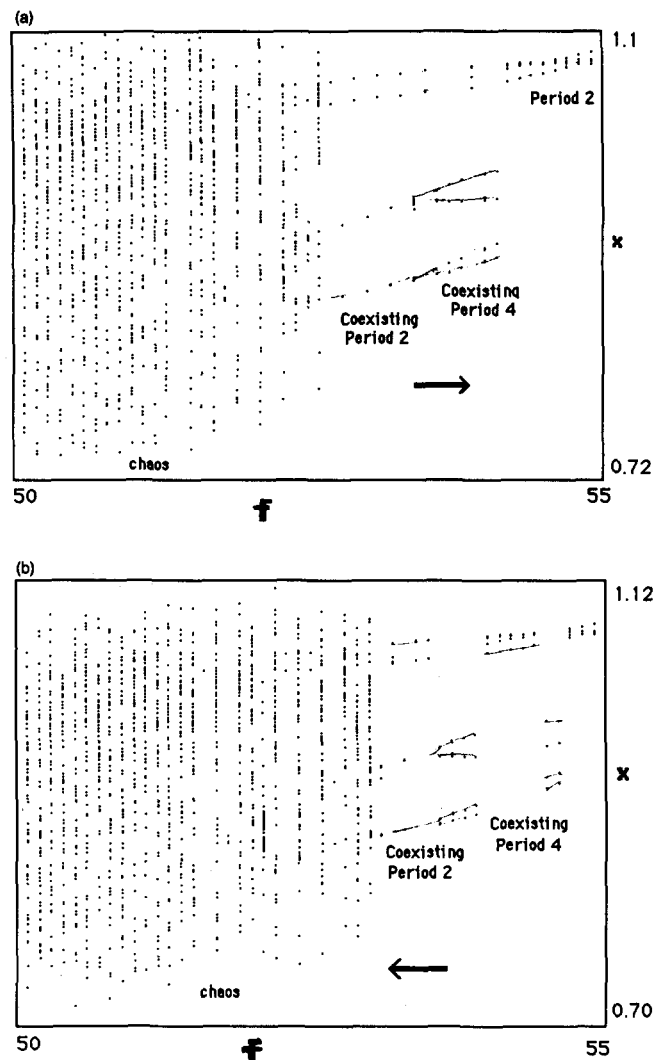


Fig. 5. Bifurcation diagram [Forcing amplitude vs $x(\tau_n)$] for circular oscillations of a vibrating string: (a) forward scan; (b) backward scan. Same operating parameters as Fig. 4; however, oscillations are not planar, but circular. Strictly planar vibrations are observed at higher forcing amplitudes.

In this way, we can study the evolution of the attracting orbits as one of control parameters is varied. Since the system shows hysteresis, the bifurcation diagram depends on the direction in which the parameter is scanned. In this study, we show the results for the control parameter being scanned in both directions.

The results for the Duffing oscillator [Eq. (20)] are presented in Fig. 4. The first bifurcation diagram, Fig. 4(a), shows the results of a forward scan, $F: 50 \rightarrow 55$; Fig. 4(b) is a backward scan, $F: 50 \leftarrow 55$. Both scans show that two period 1 orbits coexist when $F \in [54.5, 55]$. In fact, these are exactly the two orbits calculated in Sec. IV. As shown in Fig. 4(b), each of these orbits undergoes a period-doubling cascade to chaos as F is decreased from 55 to 53. This is followed by a period 3 window and then more chaotic behavior. At least two different chaotic attractors as well as a period 3 orbit all coexist in some parameter regimes between $F \in [50, 53]$.

In Figs. 4 and 5, the orbit appears to hop between attractors as F is incremented. This is an artifact of the way the bifurcation diagrams are constructed. F is incremented by

steps of 0.1, and the different basins of attraction are sufficiently intertwined so that this finite step size for F can throw the orbit onto another attractor. Even in an experimental system, F might not vary continuously in the quasi-static approximation (this is especially true for experiments under computer control), and one might observe a sudden switching between attractors in this parameter regime. If a smaller increment size is employed, the period N orbits and the chaotic attractors can be followed in more detail.

The bifurcation diagram for forced circular motion, Eq. (10), is presented in Fig. 5. Regions of period motion and chaotic motion (or possibly quasiperiodic motion) are easily distinguished. In this parameter region, all periodic motions appear to be circular [i.e., $y(\tau) \neq 0$]. Numerical studies show that a transition from planar to circular motion takes place when $F = 61.7$.

Neither of these bifurcation diagrams are meant to be an exhaustive or comprehensive study for the dynamics of a vibrating string. They merely serve to indicate that the

forced vibrations of a string can exhibit a rich variety of complicated motions under realizable operating conditions.

VII. CONCLUSION

We studied the nonlinear vibrations of an elastic string. A string is capable of exhibiting several nonlinear phenomena including periodic, quasiperiodic, and chaotic motions. Hysteresis is found using the method of slowly varying amplitudes and chaotic vibrations are predicted for forced oscillations in an experimentally accessible regime. Stable periodic vibrations exist for planar and circular motions, and a numerical estimate of the threshold for the transition from planar to circular motion is given.

This is a rich system for which the detailed comparison between theory and experiment could provide very useful insights into the nonlinear dynamics of spatially extended systems. Additional studies are possible for the subharmonic periodic orbits, as well as stability calculations showing, for instance, the transition from planar to circular oscillations. An in-depth numerical study could also facilitate experimental studies looking for specific nonlinear effects. With the onset of chaotic behavior, it is reasonable to expect that the single-mode model is not as applicable since chaotic motion can serve to excite many modes, and this suggests the formulation of a multimode model. The general question of the "excitation of multiple modes" by chaotic oscillations could be fruitfully explored by both theoretical and experimental work on vibrating strings.

ACKNOWLEDGMENTS

It is a pleasure to thank Professor Neal Abraham and Professor Narducci for extensive comments on a preliminary draft of this manuscript. I would also like to thank Bill Scharpf for several insightful remarks.

¹H. Harrison, "Plane and circular motion of a string," *J. Acoust. Soc. Am.* **20**, 874 (1948).

²D. Martin, "Decay rates of piano tones," *J. Acoust. Soc. Am.* **19**, 535 (1947).

³G. Weinreich, "Coupled piano strings," *J. Acoust. Soc. Am.* **62**, 1474 (1972).

⁴Lord Rayleigh, *Philos. Mag.* **15**, 229 (1883).

⁵P. Morse and K. Ingard, *Theoretical Acoustics* (McGraw-Hill, New York, 1968), Chap. XIV.

⁶R. Narasimha, "Non-Linear vibration of an elastic string," *J. Sound Vib.* **8**, 134 (1968).

⁷J. Miles, "Stability of forced oscillations of a vibrating string," *J. Acoust. Soc. Am.* **38**, 835 (1965).

⁸For an elementary and up-to-date introduction to nonlinear dynamics, see P. Bergé, Y. Pomeau, and C. Vidal, *Order Within Chaos* (Wiley, New York, 1984); J. Thompson and H. Stewart, *Nonlinear Dynamics and Chaos* (Wiley, New York, 1986); or P. Milonni, M-L Shih, and J. Ackerhalt, *Chaos in Laser-Matter Interactions* (World Scientific, Singapore, 1987).

⁹For some experimental ideas, see C. Gough, "The nonlinear free vibration of a damped string," *J. Acoust. Soc. Am.* **75**, 1770 (1984); D. Oplinger, "Frequency response of a nonlinear stretched string," *J. Acoust. Soc. Am.* **32**, 1529 (1960); G. Murthy and B. Ramakrishna, "Nonlinear character of resonance in stretched strings," *J. Acoust. Soc.*

Am. **38**, 461 (1965); C. Baker, C. Thair, and C. Gough, "A photo-detector for measuring resonances of violin strings," *Acustica* **44**, 70 (1980); E. Arnold and G. Weinreich, "Acoustical spectroscopy of violins," *J. Acoust. Soc. Am.* **72**, 1739 (1982); A. Lee and M. Rafferty, "Longitudinal vibrations in violin strings," *J. Acoust. Soc. Am.* **73**, 1361 (1983); J. Sandoral and A. Prota, "Fourier analysis for vibrating string's profile using optical detection," *Am. J. Phys.* **53**, 1195 (1985); G. Shanker, V. Gupta, and N. Sharma, "Normal modes and dispersion in a beaded string," *Am. J. Phys.* **53**, 479 (1985); M. Podlesak and A. Lee, "Demonstration of resonances in string instruments," *Am. J. Phys.* **52**, 470 (1984); F. Clay and R. Kernell, "Standing waves in a string driven by loudspeakers and signal generators," *Am. J. Phys.* **50**, 910 (1982); J. Jewett and J. Spadaro, "Vibrating string resonance spectra on the oscilloscope," *Am. J. Phys.* **50**, 570 (1982); M. Beatty and J. Lienhard, "Experimental investigation of the transverse vibrational frequency ratio for identical loaded and unloaded rubber strings," *Am. J. Phys.* **50**, 113 (1982); H. Hornung and M. Durie, "Stiffness corrections for the vibration frequency of a stretched wire," *Am. J. Phys.* **45**, 991 (1977).

¹⁰C. Gough, Ref. 9.

¹¹J. Elliot, "Intrinsic nonlinear effects in vibrating strings," *Am. J. Phys.* **48**, 478 (1980).

¹²G. Anand, "Large-amplitude damped free vibration of a stretched string," *J. Acoust. Soc. Am.* **45**, 1089 (1969).

¹³R. Dicke, "Stability of periodic solutions of the non-linear string," *Q. Appl. Math.* **38**, 253 (1980).

¹⁴J. Elliot, "Nonlinear resonance in vibrating strings," *Am. J. Phys.* **50**, 1148 (1982).

¹⁵K. Banerjee, J. Bhattacharjee, and H. Mani, "Classical anharmonic oscillators: Rescaling the perturbation series," *Phys. Rev. A* **30**, 1118 (1984).

¹⁶Some recent work on the Duffing equation showing nonlinear and chaotic behavior includes Y. Ueda, "Random phenomena resulting from nonlinearity in the system described by Duffing's equation," *Int. J. Non-Linear Mech.* **20**, 481 (1985); U. Parlitz and W. Lauterborn, "Superstructure in the bifurcation set of the Duffing equation," *Phys. Lett. A* **107**, 351 (1985); S. Sato, M. Sano, and Y. Sawada, "Universal scaling property in bifurcation structure of Duffing's and generalized Duffing's equations," *Phys. Rev. A* **28**, 1654 (1983); C. Hsu and H. Chiu, "Global analysis of a system with multiple responses including a strange attractor," *J. Sound Vib.* **114**, 203 (1987); E. Dowell and C. Pezeshki, "On the understanding of chaos in Duffing's equation including a comparison with experiment," *J. Appl. Mech.* **53**, 5 (1986); B. Tongue, "Characteristics of numerical simulations of chaotic systems," *J. Appl. Mech.* **54**, 695 (1987); B. Huberman and J. Crutchfield, "Chaotic states of anharmonic systems in periodic fields," *Phys. Rev. Lett.* **43**, 1743 (1979).

¹⁷A. Nayfeh and D. Mook, *Nonlinear Oscillations* (Wiley-Interscience, New York, 1979), Chap. 4.

¹⁸C. Hayashi, *Nonlinear Oscillations in Physical Systems* (Princeton U.P., Princeton, 1985).

¹⁹This is a.k.a. the method of Krylov and Boyoliubov in the mathematics and Russian communities. See Ref. 17.

²⁰This is a bit sneaky, $A = A^*$ is allowed here because there is no damping term causing a frequency shift in the approximation to first order. In general $A \neq A^*$, and then the slowly varying amplitude approximation results in both a detuning and a phase shift. Both data are encoded by $A \in \mathbb{C}$.

²¹For a linear stability analysis of these three orbits, see Ref. 17, p. 171.

²²Robert Gilmore, *Catastrophe Theory for Scientists and Engineers* (Wiley, New York, 1981).

²³C. Grebogi, E. Ott, and J. Yorke, "Chaos, strange attractors, and fractal basin boundaries in nonlinear dynamics," *Science* **238**, 632 (1987).

²⁴N. B. Tufillaro and G. A. Ross, ODE—A Program of the Numerical Solution of Ordinary Differential Equations, Bell Laboratories Technical Memorandum 83-52321-39 (1983); program and documentation are in the public domain, and are available from the first author.